Addis Ababa University

Addis Ababa Institute of Technology

African Railway Center of Excellence

Wear Analysis of Freight Train Within Different Curve Parameters

Case Study: Ethio Djibouti Freight Train

A Thesis Submitted to the School of Graduate Studies of Addis Ababa University in Partial Fulfilment of the Requirements for the Degree of Masters of Science in Railway Engineering (Rolling Stock)

BY: TINDIWENSI EDISON

Advisor: Dr. Haileleoul Sahle HABTE

JULY 2023

ADDIS ABABA, ETHIOPIA

Declaration.

I, TINDIWENSI EDISON declare that this is my original work except that which has been referenced. It has never been submitted for any prior academic award or qualification

Name: _____

Signature _____

Date……. /……./…….

Approval

The undersigned has examined the thesis entitled "**Wear Analysis of Freight Train Within Different Curve Parameters**" presented by Tindiwensi Edison of registration number GSR/7360/14, in partial Fulfilment of the Requirements for the Degree of Masters of Science in Railway Engineering (Rolling Stock).

Dr. Haileleoul Sahle	----------	----------
Advisor	signature	Date
Dr. Araya Abera Betelie	----------	----------
External Examiner	Signature	Date
Mr. Biniyam Ayalew	----------	----------
Internal Examiner	Signature	Date
Mr. Zewdie Moges	----------	----------
A/Director of ARCE	Signature	Date

Acknowledgment

First and foremost, I give praise, honors, and thanks to the Lord Almighty for the gift of life and good health throughout my research work and am very grateful to the African Railway Centre of Excellency, Addis Ababa Institute of Technology, and Addis Ababa University for sponsoring my studies and research. My sincere appreciation to my advisor Dr. Haileleoul Sahle for the invaluable guidance, and motivation throughout this research work. I cannot thank you enough for your endless assistance and advice. Special thanks to Mr. Awel Mohammed for your immense knowledge, motivation, unconditional assistance

This thesis is wholeheartedly dedicated to my loving parents who have been a constant source of support and encouragement throughout my academic career and life. You have always believed in me and pushed me to reach for the stars. Your unwavering faith in my abilities gave me the confidence I needed to complete this project. I also dedicate this work to my brother Benjamin who has never stopped cheering me on every step of the way. You were always there to listen and offer advice when things got tough. Thank you for being my rock. To all my relatives - your care and interest in my work inspired me more than you can imagine. You always reminded me that family comes first. I could not have completed this thesis without the foundation that each of you provided in your own way. From the bottom of my heart, I thank you all.

ABSTRACT

This research deals with wear analysis along the Ethio Djibouti freight train under different parameter conditions. The main focus of this research is to understand how different parameters influence wear along the curve during operation, considering the effect of supervision, curve radius, and curving speed after a given distance of operation, such as 20000 km. The measured wear rates strongly correlate with superelevation. Below the equilibrium cant, wear rate rises exponentially as cant deficiency increases. However, further increasing cant beyond equilibrium provides diminishing wear rate returns. This research enhances the fundamental understanding of wheel-rail wear mechanics in curves and provides validated tools to predict and mitigate wear.The results show that when the above distance is run under different curve radius creep, the wear volume increases from 6.8 mm to 3.7 mm as the radius increases from 600 to 1200 m, especially on the outside wheels. Wear increased from 6.6 to 7.8 mm as the speed increased from 40 to 100 km/hr. after a distance of 20000 km. Increasing the superelevation from 80 to 140 mm reduced wear due to improved curves from 7.1 to 6.7 mm after 20.00 km, and a significant decrease in wear volume from 8.9 to 2.3 mm outside wheels after a 20.00 km operational distance.

Keywords: multi-body analysis, Archard law, wear model, curved track, superelevation,

Table of Contents

List of Figures

List of Tables

List of Abbreviations

RRD	Rolling Radius Difference
EDR	Ethio-Djibouti Railway
FCG	Fatigue Crack Growth
MBS	Multibody System
EN	European Standard
DOF	Degrees Of Freedom
COF	Coefficient of friction

List of Acronyms

K	wear coefficient
h_t	Maximum Superelevation
V	Operating Speed of Vehicle
R	Curve Radius
y	Lateral Displacement
T_x	Longitudinal Creep Force
α_t	
Q	Vertical Force
H	The hardness of the material
S	sliding distance
W_{vm}	Wear Volume
WS1L	Left Wheel is one of the first wheelsets
WS1R	Right Wheel one of the first wheelset
WS3L	Left Wheel one of the third wheelset

Chapter1: INTRODUCTION

Railway history in Ethiopia can be traced way back a century with the construction of a 784 Km railway in 1917 linking the capital Addis Ababa with the port of Djibouti[1] but the operation was phased out (disrupted) due to the absence of maintenance and repair. The line had reached Akaki, only 23 kilometers from the capital city by 1915, and two years later came to Addis Ababa itself[2]. This marked the official commercial opening of the 784 km long railway, although the Station of Addis Ababa was not inaugurated until 3 December 1929. The Ethio-Djibouti Standard Gauge Railway (EDR) was established in April 2017 to better logistics and transportation connectivity between the two countries. This project was expected to be able to drive the economic growth of Ethiopia. This is because the import-export of Ethiopian commodities was wholly dependent on the port of Djibouti. This can be said because at least 95% of Ethiopia's Import & Export trade transits through the Port of Djibouti with only limited trade through Port Sudan.

Figure1. 1: Ethio Djibouti Freight Train[3]

Ethiopia is one of the few African countries with an established railway system with a freight railway associated with wheel and rails, especially wheel flange wear and rail side wear on curves due to the poor topography[4]. With the increase in train speed ed the wheel-rail interaction increases inevitably hence severe wheel-rail dynamic interaction will cause severe wear of wheels and rails[5]. Therefore, this is a major attribute affecting the safety of the rail vehicle, which when not addressed extensively may result in accidents as a result of derailments

1.1: Background of Research

Wear is referred to as the removal of material contacting solid surfaces in relative motion with each other[6]. When Wheel-rail surfaces are subjected to contact, stress results in surface damage, which is observed as either wear or damage mechanisms. It is one of the most critical issues affecting the cost and performance of railway transportation systems[7]. It has a very large effect on vehicle dynamics, so excessive modifications of the original wheel have to be removed by grinding and re-profiling the wheel to its original profile.

The freight railways are mainly composed of tangent tracks and large curved tracks, and the performance between the wheel tread and rail has improved by wheel profile optimization[8], [9]. However, the sharp curves exist along the tracks and towards the yards, and the flange wear caused by it cannot be ignored [10]. The main reason for wheel flange wear is due to stress concentration caused by the contact between the wheel flange and the rail gauge corner. A large wheel flange force under a sharp curve of 1,200m for a normal section and 800m for a difficult section will inevitably cause severe wheel flange wear and side rail wear which becomes the decisive factor for rail replacement on a curved track[3].

Wheel/rail wear problems have become serious, especially in terms of circular wheel wear and hollow tread wear[11]. Severe wheel tread wear causes an increase in wheel flange height and running resistance; it can also affect vehicle stability and ultimately can lead to derailment. Once a wheel is worn or otherwise damaged, it must be reprofiled to recover the standard profile of the wheel flange and tread. Reprofiling is expensive, and the amount of metal removed from the

tread surface during the cutting process is often greater than the amount of metal lost to wear [11]

Figure1. 2:Wear on the wheel

Even if, the results and findings of the studies aim at predicting wear of the wheel-rail they mainly focus on wear majorly on straight trucks but limited wear along curves at different radii and other parameters like cant, superelevation, critical speed, critical height, and transition length among others[12],[13].

The spalling defect is the major defect, especially on the inner rail along sharp curves which is mainly distributed in the center region of the rail top. With a continuous expansion in the railway traffic volume, the wear rate presents an upward tendency. Therefore, it is of significance to make a deep investigation into the rail wear mechanism and to seek technical measures to alleviate the rail wear in heavy-haul railways

Therefore, understanding the real cause of failure and wear under curves along the Ethio Djibouti railway line will help to predict failure rates and maximize the performance of the freight transport along the line and more so improve the railway systems in the future.

1.2: Problem Statement

Rail wear is a significant issue for freight train operations, leading to high maintenance costs and safety concerns. Wear rates are experienced on curve sections of the track due to the additional friction and forces acting on the wheel-rail interface. The radius and superelevation of curves have been shown to impact wheel-rail contact conditions and subsequent wear, however, further analysis is needed to fully characterize these effects. This thesis aims to conduct an in-depth study on curve parameters' effects on freight train operations wear rates. Specific curve features to be evaluated include radius and superelevation imbalance. Field measurements and simulations will be used to model different curving conditions and predict wear for CW4 Open Top Wagon. The expected outcomes will be an improved understanding of the relationship between freight train curving behavior and wear, identification of curve design guidelines to minimize wear, and estimation models to predict wheel and rail life under various curving parameters. The results will provide valuable insights to help rail infrastructure managers and freight operators optimize curve maintenance practices, extend asset life, and improve safety for freight rail networks.

1.3: Research Questions

The following are the questions that this study quest to answer.

- What radius limits provide the lowest wear rates?
- Is there an optimal curving speed that minimizes wear?
- Can balancing superelevation reduce wear rates?

1.4: Objectives

1.4.1: Main Objectives

This study aims to study the effect of different curve parameters on the wheel wear of the Ethio Djibouti freight train.

1.4.2: Specific Objectives

- To analyse the effect of radius of curvature on wear along the Sebeta-Adama Ethio Djibouti rail transit.
- To analyse the effect of different vehicle speeds on the 1000m curve along Ethio Djibouti rail transit.
- To analyse the effect of superelevation on wear along the Ethio Djibouti rail transit.

1.5: Scope and Limitations

The study will focus primarily on wear analysis of wheels and rails, not other train components. Field measurements and simulations will be limited to standard freight wagon types commonly used for bulk commodities, intermodal, etc. Passenger wagons are excluded and Study is focused on dry conditions. Effects of lubrication, moisture are not addressed.

1.6: Significance of the Study

Curve-induced wheel and rail wear presents a costly maintenance and safety issue for railways. This thesis investigates the impacts of curve parameters like radius on wear through field and simulation studies of freight curving. It aims to define infrastructure and wheel-rail interface guidelines to optimize asset life, operations, and safety. Despite a limited scope, the expected academic and practical contributions merit research on this topic. The work will provide fundamental insights and models to help railways minimize curve wear rates, safety impacts, and lifecycle costs.

Chapter2: LITERATURE REVIEW

2.1: Introduction

This section comprises a review of different studies related to wear. It gives a review of the previous research that has been carried out about wear but specifically along curves. Some recent research in this area includes; the wear process which includes consideration of the different theories used like the Archard wear majorly and contact mechanics, which involves forces and relative motion between the wheel-rail contact key components in determining the wear performance.

2.2: Theory of Multi-body system dynamics

A computer model is created by preparing mathematical equations that represent the vehicle-track system. These equations are typically second-order differential equations that can be combined into matrices. The computer package automatically prepares these equations, which can be collected through a user interface or by entering data about the vehicle's body and suspension components. The complexity of the system can be varied to suit the simulation and the desired results. Physical constraints may limit the system's movements, and the system can be simplified accordingly. The application of constraint equations results in ordinary differential equations (ODE) or linear algebraic equations (LAE) and ODEs, depending on the application method.[14]. Some various coordinates and formalisms lead to suitable descriptions of multi-body systems. In this work, the methods presented in SIMPACK are based on the use of Cartesian coordinates, which lead to a set of differential-algebraic equations that need to be solved. It is assumed that appropriate numerical procedures are used to integrate the type of equations of motion obtained with the use of Cartesian coordinates. It is also assumed that the various numerical issues that arise from the use of this type of coordinates, such as the existence of redundant constraints and the possibility of achieving singular positions, are also solved. A typical multi-body model is defined as a collection of rigid or flexible bodies that have their relative motion constrained by kinematic joints that are acted upon by external forces. Let the multi-body system be made of N number bodies. The equations of motion for the system can be described as

$$M\ddot{q} = \mathrm{g}. \qquad (2.1)$$

Where M is the mass matrix, which includes the masses and inertia of the individual bodies, q is the vector of generalized coordinates and correspondingly q̈ is the acceleration vector, and g is the vector with applied forces and gyroscopic terms.

2.3: General Wheel-Rail Interaction on Curves

A railway wheelset is made up of two wheels connected by a rigid axle. The railway wheelset has developed over time, but the basic design has stayed consistent. Iwnicki [15]gives a historical review of the development of the railway wheelset. By the matching design of wheel-rail contact geometry, the rail-grinding profiles with good contact geometry state may be acquired. However, another important issue that must be paid attention to is the actual wheel-rail dynamics performance of a heavy-haul freight vehicle passing through a curved track with the designed rail-grinding profiles. Here, the wheel-rail lateral force is a key factor, which is mainly responsible for the rail side wear. On the curved track, the wheelset is steered by the lateral forces acting on wheels, which mainly depend on the longitudinal creep forces $(F_{x\mathrm{Li}}, F_{x\mathrm{Ri}})$ and the lateral creep forces $\left(F_{y\mathrm{Li}}, F_{y\mathrm{Ri}}\right)$, as shown in Figure (2.1) If the wheel and rail profile are designed to be able to provide enough RRD, the creep forces will push the wheelset to adjust the radial position without wheel flange contact. Conversely, small RRD results in a large attack angle of the wheelset, and the wheel flange usually contacts the rail side. Once the wheelset is steered by the wheel flange, severe rail side wear may happen.

The primary concerns of railway pioneers in the early days were reducing rolling resistance and wear while boosting strength. To achieve this, the wheel tread was added to prevent rubbing of the wheel flanges on the rail gauge face. When a coned wheel moves laterally from its equilibrium position, a rolling radius difference is created, which causes wheeled steering around a curve. This difference creates kinematic oscillations or instability on tangent tracks, according to Iwnicki. This was described by Klingel theoretically described in 1883. It was noticed that a wheelset must radially align itself on a curve to maintain pure rolling.

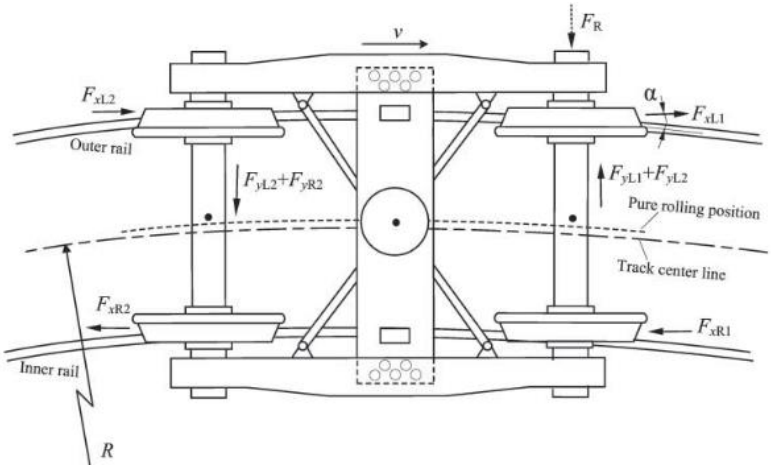

Figure 2. 1. Basic wheel-rail forces acting on the bogie in a curve[16]

2.4: Movement of Vehicle on Curved Track

The curved track is either horizontally curved track or canted based on the introduction of super elevation on the track to counteract the lateral centrifugal force developed due to the curving movement of the vehicle by lateral centripetal force. A horizontal curved track is constructed on a level horizontal plane without an introduction of super elevation while a canted track is constructed with the introduction of superelevation. The curving motion of the vehicle on a horizontal track or canted track is accompanied by wheelset lateral movement.

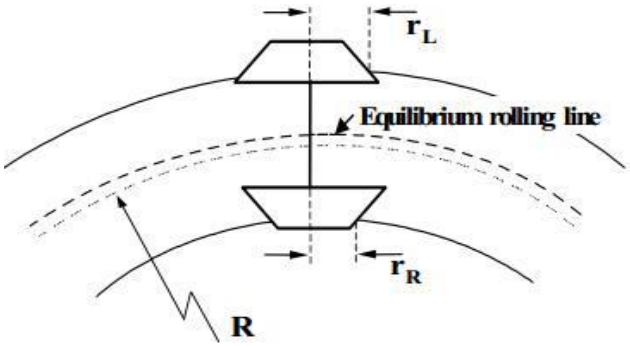

Figure 2. 2: Rolling radius difference between inner and outer rail[17]

A wheelset radially aligns itself in a curve to sustain pure rolling as from a coned wheelset in a curve. This analysis was only based on the geometrical relationships of an unconstrained

wheelset negotiating a curve as seen in Figure 2.3 It was established that the lateral displacement (y) required to sustain pure rolling is a function of the radius of the curve(R_c), the nominal radius of the wheelset (r_o), the distance between the two contact points and the conicity (λ) of the wheels as shown in equation[15], [18]. This relationship shows that the ability of a wheelset to roll freely around a curve is dependent on the conicity of the wheelset.

$$y = \frac{r_o l}{R_c \lambda}$$

(2.2)

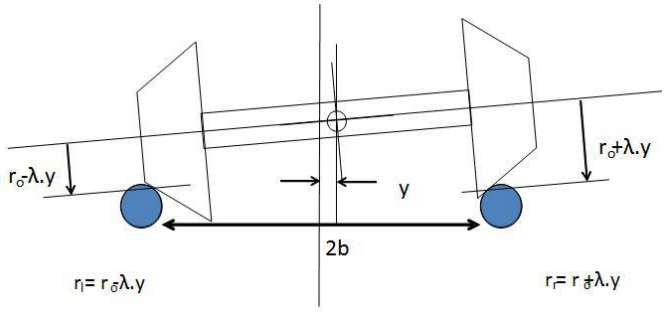

Figure 2. 3: Inner and outer rail of a track[18]

2.5: Mathematical Analysis of Vehicle on a Curve

If a vehicle having mass M (weight W) is moving on a curve of radius R with a speed V, the centrifugal force experienced by the vehicle comes to $\frac{mv^2}{R}$. This force is acting at the center of gravity of the vehicle in a perpendicular direction away from the center of the curve. If the curve is having a cant, centripetal force will be acting towards the center of the curve. When the two forces acting in the lateral direction match with each other, the vehicle is in equilibrium as far as lateral forces are concerned. In this situation, any person sitting inside the vehicle will not be able to differentiate between the motion on a straight or a curve due to the absence of lateral forces. The cant at which the equilibrium is there on a curve is called equilibrium cant. Conversely, the speed corresponding to cant in any curve is called equilibrium speed. By assuming the two forces (centrifugal and centripetal forces) are equal, the relation between equilibrium speed and equilibrium cant can be designed

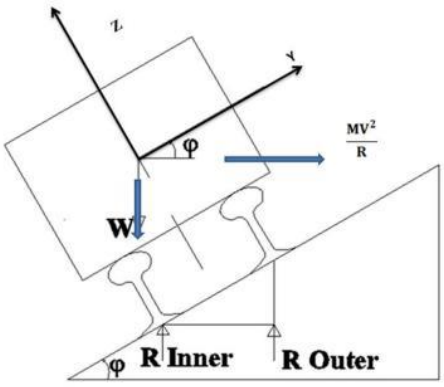

Figure 2. 4: Forces on the vehicle on the canted curve [19]

In the literature, considerable research is performed in different areas related to this research. Some of the research has a direct relation to this study whereas others have indirect relations. Wear is the process leading to the loss of material from one or more solid surfaces in a sliding, rolling, or impact motion relative to one another. As with friction, wear is not a material property, it is a system response. It is common to divide wear seen in the field into three regimes: mild, severe, and catastrophic.

The wear of wheels and rails, especially the wheel flange wear and the rail side wear on curves, is a long-standing problem of heavy-haul railways. With the rise in train speed and transport capacity, the wheel-rail interaction aggravates inevitably. Studies show that the predominant wear is the side wear of outer rails on small radius curves. In a curve or transition curve, the flange might be in contact with the gauge corner of the rail head, and sliding interactions can become predominant. As the curve radius rises, the outer rail side wears increase rapidly.

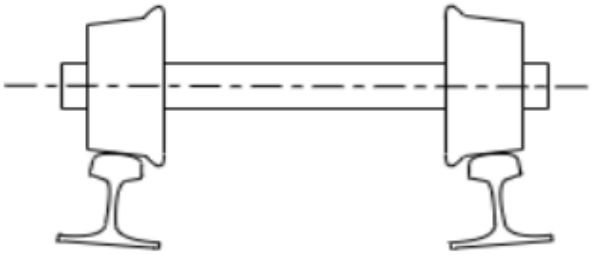

Figure 2. 5: Contact between rail and wheelset on straight track

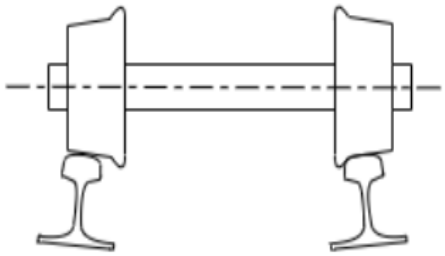

Figure 2. 6: Contact between rail and wheelset on a curve [20]

As a result of the above discussion, lubrication at the wheel flange and rails on sharp curves has been commonly adopted as a method of reducing friction between the wheel flange and rail gauge face to minimize wear and energy consumption. Many friction models show that friction is affected by the theology of the third body, slip distance, and load with the shear stress, of which slip distance exhibits the dominant influence[19].

In curves, there can be a large sliding component on the contact patch at the gauge corner of the rail head since the wheel flange is in contact with the gauge corner of the rail and nearly conforms to the flange shape. The wheel-rail contact under this condition usually leads to an incremental load on the rail side. With a continuous expansion in railway traffic volume, the wear rate presents an upward tendency. A vehicle passing through a curved track will experience a lateral force. This wheel-rail lateral force is a key factor, which is mainly responsible for the rail side wear. On a curved track, the wheelset is steered by the lateral forces acting on the wheels. If the wheel and rail profiles are designed to be able to provide enough rolling radius difference, the creep forces will push the wheelset to adjust the radial position without wheel flange contact. Conversely, a small rolling radius difference results in a large attack angle of the wheelset, and the wheel flange usually contacts the rail side[20]. Once the wheelset is steered by the wheel flange, severe rail side wear may happen. On sharp curves, the outer rail profile with severe side wears nearly conforms to the flange shape.[14]. Lubrication sharp curves are

considered an effective solution for reducing wear loss of material from the effective cross-section of rail and wheels. Rail administrations around the world have been increasing axle loads and traffic densities in rail networks.

When studying wheel-rail contact conditions, it is worth mentioning some of the traditional theories which have led to this day's transformation. The theories are divided into two[21], which are normal and tangential contact theories. For normal wheel-rail contact problems, the best-known analytical method is the Hertzian theory established by Heinrich Hertz in 1882. Hertz's theory has been commonly utilized due to its reasonable accuracy in most wheel-rail contact situations. The geometry of the contact zone and the distribution of contact pressure can be determined from this theory. Hertz's theory is based on some assumptions [22].

Therefore, this section comprises a review of different studies on the wear of railway rails. One of the importance of studying rail wear is to improve the safety of the railway infrastructure and also reduce operational costs. Some authors[23],[24], [25] have studied the wear of railway rails and [26]–[28] have studied the wheel-rail wear along curves but according to Dirks [22] found that the location of the highest wear on rails depends on whether the rail is located in a curve or on a straight track. Two examples of what worn rails can look like are shown in the Figure below which shows worn profiles as dashed bars. In a curve, the rail is exposed to higher creep forces and creepages and will show more wear. Since the wheel-rail contact on the outer (high) rail in a curve is located at the gauge corner, the highest wear will take place here as well.

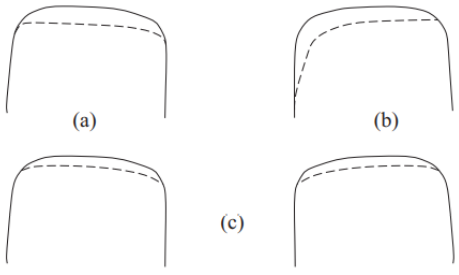

Figure 2. 7: (a) inner (low) rail in a curve, (b) outer (high) rail in a curve (c)on a straight truck [24]

For the inner rail in a curve, the highest wear will be located on top of the rail. For rail profiles on straight track, the wear will be more evenly distributed on the top and at the gauge corner, mainly due to irregularities in the track and the wear rate can be reduced by applying track-side lubrication in sharp curves.

The rail wear along curves has been studied extensively and the results show that rail wear is more severe on small radius curves, compared to larger ones and it picks the optimal parameter combination, which may decrease wear[29]. The degree of wear depends on many parameters such as horizontal curve radii, type of vehicle bogies, lubrication, etc. Wheel wear is not only a maintenance problem but also significantly affects the vehicle's dynamic performance in terms of safety against derailment, dynamic stability, ride comfort, etc. It is therefore of interest to investigate how wheel profiles change due to wear over time for various railway applications[5]. When a vehicle is traveling on a highly curved rail track, the wheel and rail make two contact patches between the wheel tread and the rail, and between the wheel flange and the rail gauge corner. This scenario causes material loss from the contacting components, which leads to wear of the wheel tread and flange[30]

2.6: Modeling of Wear rate

The wear that inevitably occurs between the wheel and the rail while the vehicle is moving along curves depends on a large number of factors, among which sliding phenomena inside the contact patch, the normal force transmitted, the friction coefficient, size and shape of the contact patch, etc. Wear on wheels and rails makes it necessary for the wheel to be replaced when the upper safety limits have been reached because the vehicle also sustains losses in terms of dynamic performance. Worn profiles tend to be less stable and show lower performance levels when negotiating curved tracks, and this makes reducing the wear index a major factor in the design of railway vehicles. At present, several models are attempting to quantify the wear index that includes some of the abovementioned parameters.

Most used theories in railway dynamics assume that wear is proportional to the energy dissipated within the contact patch, calculated as the scalar product of tangential force on the contact and

the value of creepage. Models assume the material loss is proportional to the frictional energy dissipated in the contact patch ($T\gamma$). Tγ is expressed as the sum of the products of the creepage and creep force for the lateral, longitudinal, and spin components, as illustrated below:

$$\mathrm{T}\gamma = \left[T_y\gamma_y\right] + [T_x\gamma_x] + [M_z\omega_z] \tag{2.3}$$

Where T_y, T_x are lateral and longitudinal creep force respectively, and M_z is spin creep moment. γ_y, γ_x are lateral and longitudinal creepages, and ω_z is spin creepage, the spin creepage contribution is dismissed; the result is called the wear number.

2.6.1: The wear models

Archard's wear model [31]is based on the assumption that the volume of removed material is proportional to the dissipated energy. The dissipation of energy is the work done by frictional forces so wear is only present in the sliding part of the contact. This model is derived using the theory of asperity contact and was first done by Reye in 1860 [32]. The Archard equation for the wear volume is as follows

$$\mathrm{V_{wear}} = \mathrm{k}\frac{\mathrm{Ns}}{\mathrm{H}} \tag{2.4}$$

The wear volume is proportional to both the normal force, N, and the sliding distance, s. H is the hardness constant of the softer material and k is a wear constant normally ranging from 10^{-8} to 10^{-2}. The magnitude of the loading, the material, and the local friction are typically the factors influencing k.

2.6.2: Contact problem calculation methods

The linear theory cannot be used to calculate wear because it assumes no slip, which is required to calculate wear. To address this issue, Kalker developed the FASTSIM algorithm[33], which only works in Hertzian areas. Apart from calculating frictional stresses according to Kalker's simplified theory, it is also used as a post-processor to evaluate the division of the contact area into adhesion and slip.

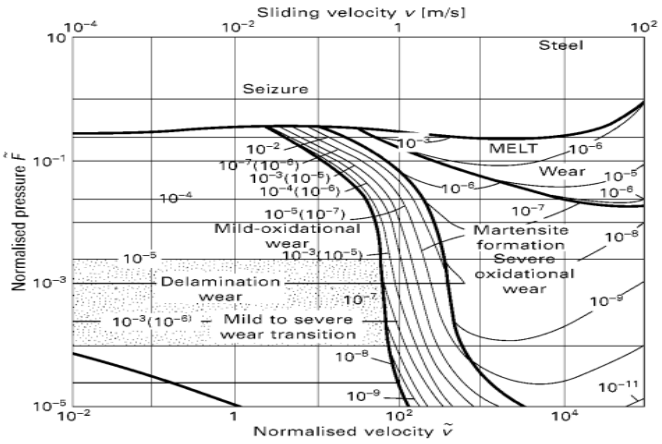

Figure 2. 8: Steel-on-steel wear sliding wear map [34]

to apply an adequate and appropriate wear coefficient wear map recognize as a good approach to take. The wear map shown in Figure2.8, explains four approximate regions wherein the wear coefficient differs. The wear map shows the particular region where tread and flange contact occur, the contact pressure limit at 0.8H equivalent to 80% of the hardness, whereby the wear coefficient depends solely on the size of the sliding velocity. In the first region, for low sliding velocity, the wear coefficient is small. In the region between 0.2 and 0.7 m/s, the wear coefficient raises. As sliding velocity surpasses 0.7 m/s the wear coefficient, even so, reduces to the early low level. Just above the limit of 0.8H, the wear coefficient is 10 times the maximum value underneath the limit, which makes wear conditions severe.

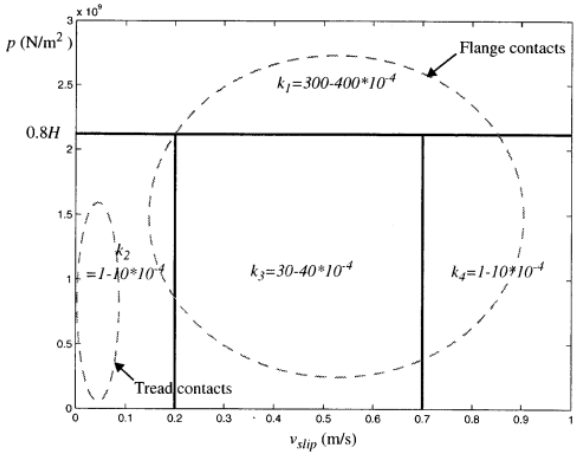

Figure 2. 9: Archard Wear Map - Wear Coefficients for Tread and Flange Contact [35]

The wear that inevitably occurs between the wheel and the rail while the vehicle is moving depends on a large number of factors, among which sliding phenomena inside the contact patch, the normal force transmitted, the friction coefficient, lubrication conditions, the size and shape of the contact patch, etc. Wear on wheels and rails makes it necessary for the equipment to be replaced when the upper safety limits have been reached and, as a general rule, the vehicle also sustains losses in terms of dynamic performance. Worn profiles tend to be less stable and show lower performance levels when negotiating curved tracks, and this makes reducing the wear index a major factor in the design of railway vehicles [36].

2.7: Wear on the wheel and rail interaction

Wear is the principal cause of rail replacement on almost all railroads. Wear tends to be concentrated on the high rail gauge face (i.e., the inner edge of the outer rail in curved track) where contact is made with the wheel flange. In straight track and large radius curves, vertical wear of the head is seen. If the rail wears severely, the stress in the rail rises, particularly in the head, and, eventually, the rail needs to be replaced. All railroads have different criteria for removing worn rail, but often these criteria imply replacement when about 30 to 50% of the head area has been lost[37].

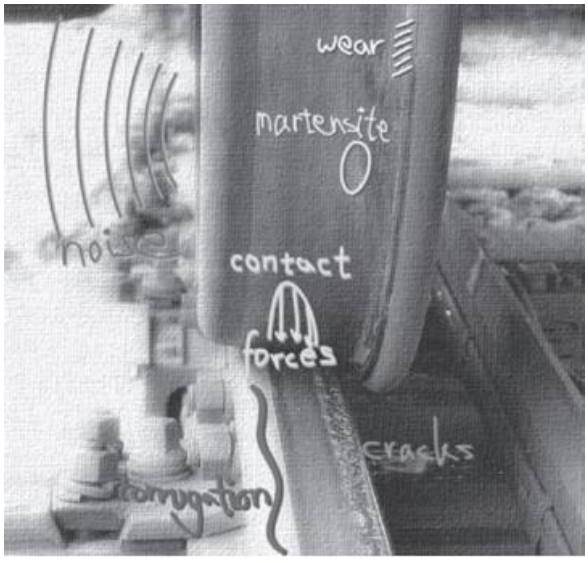

Figure 2. 10: Wheel and rail interaction[38]

2.7.1: Analysis of Factors Affecting Wheel Wear Loss.

Railway line parameters, such as curvature and superelevation, directly impact the wheel/rail contact relationship. To better reflect the random characteristics of wheel/rail matching, data is randomly sampled to generate sample vehicle speeds. The weight coefficient is assigned to a wear loss calculation model based on the probability distributions between operations at varying degrees of curvature and speed.

2.7.2: Effect of Different Curves on Wheel Wear.

To determine the optimal wheel profile in actual line operation, parameters of a freight train, including right- and left-hand curves, curve radius, superelevation, and other curve parameters. For simulation purposes, curves on the railway lines will be classified. The percentage of a tangent, spirals, and curve body associated with each curve will be calculated.

2.7.3: Effect of Speed on Wheel Wear.

The range of operating speeds in curves will be calculated based on the curve parameters and the speed distribution of vehicles in actual operation on a train. According to the 3σ rule of normal distribution[11], the different speeds and different curves will be compared with the normal distributions to show the wear distribution of the leading wheel at different velocities for the curve.

2.8: Related Research

Wang et al.2022 [39] optimized the design of railway curves to reduce wheel and rail wear using multi-objective genetic algorithms. Optimal solutions were provided for radius, cant deficiency, and speed.

Zhao et al. 2020 [40] used a coupled multibody dynamic, contact mechanics, and wear modeling approach to evaluate the impacts of traction and braking forces on curved track wear rates. Pellegrini et al.[41] (2015) combined multibody simulation with wear experiments on a twin-disc test rig to assess different wheel profiles and materials under curving conditions.

Several types of research studies have been made on the wear of railways under different curve parameters. Taylor and Wu 2020[27], calculated vehicle curving performances with different wheel and rail profiles and predict the evolution trend of the wheel and rail wear. J. Wang et al. 2015[20] found that a high-order transition curve and extending the transition curve length can improve the railway vehicle's driving performance on the curve and reduce the curve rail wear.

Dirks 2015[22] studied the measurement of the wheel on rail fatigue and wear using the wear and rail contact fatigue (RCF) models and the objectives were to gain insight into the causes of the wear and RCF damage and also obtain an overview of the existing wear and WRC models. He found the highest wear on rails depends on whether the rail is located in a curve or on a straight track and it exists on the outer rail of the curve on the gauge corner.

Ye et al. 2021[42] used Hertz's theory to solve the wheel-rail normal contact problem and FASTSIM to solve the tangential contact problem. Different wear modeling approaches were discussed, mainly based on the proportionality of wear with the energy dissipated at the contact. To be able to compare data and numerical results, a smoothing procedure was applied to the updated wheel profile.

Stuart L. 2021[9] provided a model of wheel wear based on the relationship between longitudinal and lateral primary suspension stiffness and the coefficient of friction at the center plate between the wagon body and the bolster, and they discovered a significant increase in wheel wear with increasing longitudinal primary suspension stiffness. Yang et al. 2016[43]studied the relationships between wear depth and . The results showed that wear depth was significantly influenced.

Telliskivi and Olofsson 2015)[44] pointed out that the matching of worn wheel and rail profiles would easily lead to the contact between wheel flange and the inner side of the rail, which intensified the rail side wear.

2.9: **Summary of Literature**

Many important research papers have been published on wear based on global and local approaches for wear evaluation, with others focusing on the effects of structural flexibility on wear models. The summary of reviewed papers based on the objective, methodology, and findings is shown in Table 2.1 below. There hasn't been much research so far done by scholars about the Ethio Djibouti freight train more so on how different parameters influence wear. This research aims to present a complete model for the prediction of wear along the curves that involves multibody simulations and Archard principles, curve radius, superelevation, and on wear and helps to come out with the best parameter that produces the least wear during operation. The model also addresses the effects of vehicle speed on wheel wear along a curve.

Table 2. 1:Summary of Literature Review

Author	Objective	Methods	Findings	Research gap
Dirks 2015	Development of a wheel-rail life prediction tool concerning both wear and surface-initiated RCF	Hertz and FASTSIM for contact modeling	The location of the highest wear on rails depends on whether the rail is located in a curve or on a straight track	Considered only the dependent on the forces applied to the wheelsets through this interface
Li et al. 2016	Investigate the rail wear on the curves of a heavy-haul line through field numerical simulations.	Archard law for wear modeling Non-Hertzian contact model	Fluctuation of wheel-rail forces throughout the curve is the main cause of the wear	Assumed that the rail material is homogeneous
j. Kim, J. Kim, and D. Kim 2023	Compare simulation findings with measurements to forecast wear of two types of wheel profiles S1002CN, S1002CN	Hertz and FASTSIM for contact modeling	Wear volume increases with increasing velocity, decreasing radius of curvature, and decreasing lubrication	Lack of a comprehensive wear model that can be used to predict wear in a variety of conditions
Yang et al. 2016	To study the relationships between wear depth and	Non-hertz for contact modeling Wheelset as flexible	The results showed that wear depth was significantly influenced by	Previous methods never considered numerical methods that takes in account

				of wear tread
Telliskivi and Olofsson 2015	Contact mechanics analysis of the wheel-rail contact	Hertz's analytical method Finite element (FE) code ANSYS	matching of worn wheel and rail profiles would easily lead to the contact between wheel flange and the inner side of the rail	The limit of the half-space assumption used in Hertz and Contact methods needs more study
Jendel et al.2002	Wear depth after 200,000km	FASTSIM for contactmodelling Archard law	The wear depth after200,000km is 2 mm	Experimental validation needed. Single curve radius analyzed.
Pereira, 2010	To study the influence of primary suspensions on wear devolvement	Energy dissipated wear modelling Wheelset as rigid structure	The results reveals that the vehicle arranged with the softer primary suspension produces less tread and flange area wear	Field validation needed. Limited to tread braking wear.
Baeza et al, 2011	To influence of flexible wheelset on wear depth	Non-hertz and FASTSIM for contact modelling Frictional work for wear modelling	Depths estimated using the rotating flexible wheelset are much higher than those predicted by using the rigid wheelset model	Limited study for a single wheel profile and operating condition.

From the above literature its seen that there hasn't been much research so far done by scholars about the Ethio Djibouti freight train more so on how different parameters influence wear. This research aims to present a complete model for the prediction of wear along the curves that involves multibody simulations and Archard principles, curve radius, superelevation, and on wear and helps to come out with the best parameter that produces the least wear during operation

Chapter3: METHODOLOGY

3.1: Introduction

The rigid model of a freight train was established, and the vehicle system included a car body, bogie frames, and wheelsets, to take into account the effect of various curve parameters on the wear. In the aspect of dynamic simulation, the results consistent with the actual situation will be obtained by wear simulation based on the Archard wear model, to provide the reference for future wheel-rail wear simulation [45]. Using the FASTSIM algorithm and the methods of simulation analysis, the influences of curve radius, superelevation, and will be studied. The simulation analysis will be conducted on the different wear degrees of wheel-rail profile, concluding the influence of the law of wear tread of dynamic performance and the dynamic simulation software will be used to conduct simulation analysis under different curve radii, , and superelevation [46].SIMPACK will be used to conduct the simulation and analysis of the influencing factors like vehicle speed, curve radius, superelevation, and , putting forward the method to reduce the wear by optimizing the corresponding parameters

In this project, wheel wear prediction involves an iterative coupling between an Ethio-Djibouti vehicle model developed using commercial multi-body simulation (MBS) software SIMPACK and Archard wear model. In Figure 3.1, the flow chart of the iterative process is demonstrated, During the simulations, the multibody model continuously exchanges data at each time step with the Archard model, passing the wheelset variables' contact points, the wheel-rail contact forces, and the creepages, which are evaluated through the FASTSIM algorithm. Once the multibody simulations are completed, the removed material depth and its distribution along the wheel profile are obtained. Finally, the wheel profile will be updated and used for new wear calculations.

3.2: Methodology Chart

The chart shows the corresponding steps followed during the analysis of the effect of the different parameters on wear around the rail curve

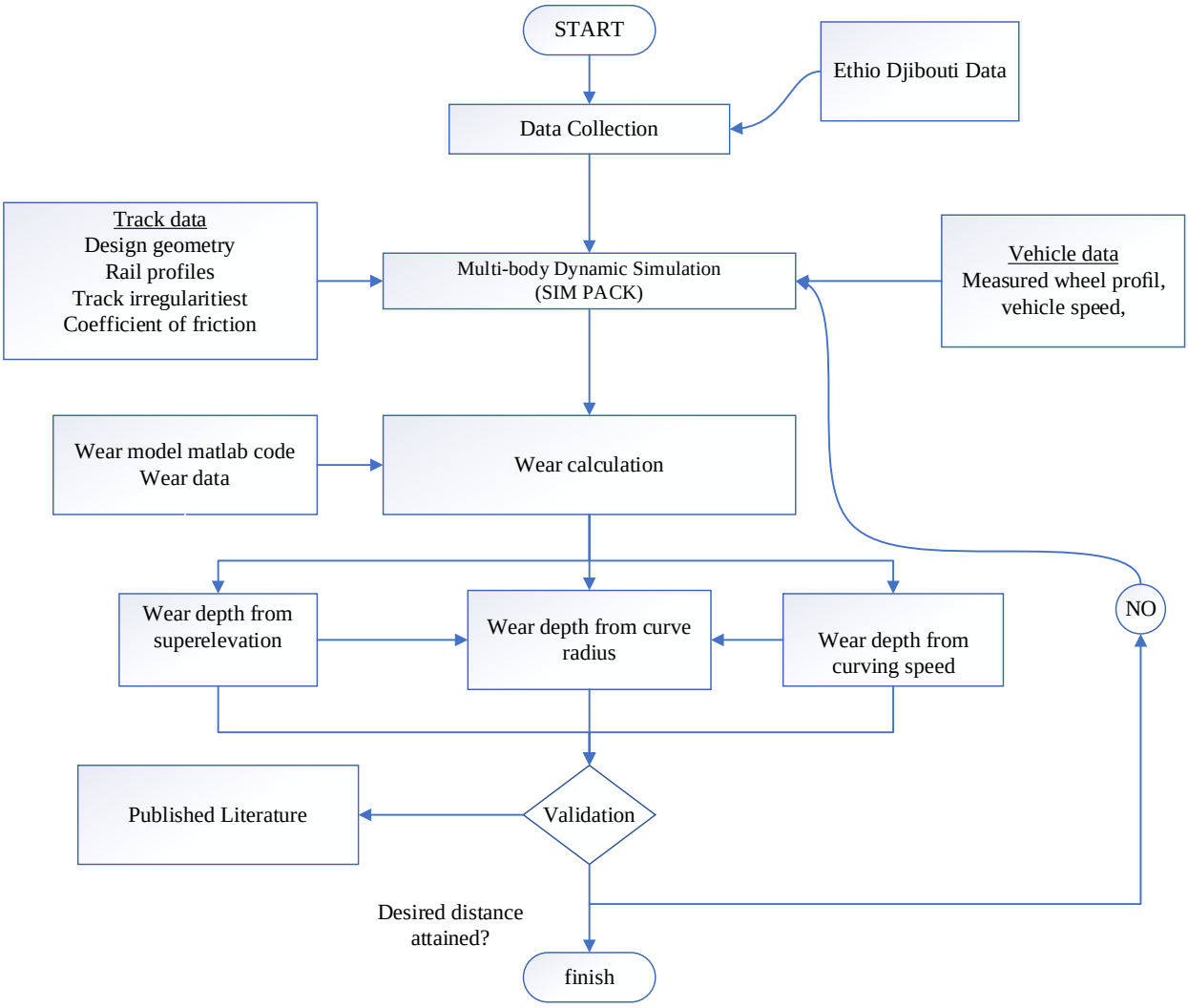

Figure3. 1:Flow chart of wear calculation

The required data that included data for the car body, the truck, and other technical parameters were collected from the Ethiopian cooperation which was used in the modeling of the Carbody and all its respective components using SIMPACK software. The model was validated where the

static force was equivalent to the dynamic force when there were no track irregularities run at a speed of 50km/hr.

Track irregularities and the Archard wear coefficients were added to the model to monitor the performance of the various parameters going to be analyzed. The specific objects were analysed independently and from the preprocessor results under the wear section the various parameters for the wear calculations were extracted and used as inputs to the MATLAB code that was programmed to calculate the wear depth

3.3: SIMPACK Train model.

The commercial dynamics Software Simpack was used to design the model train using the above parameters gotten from ERC

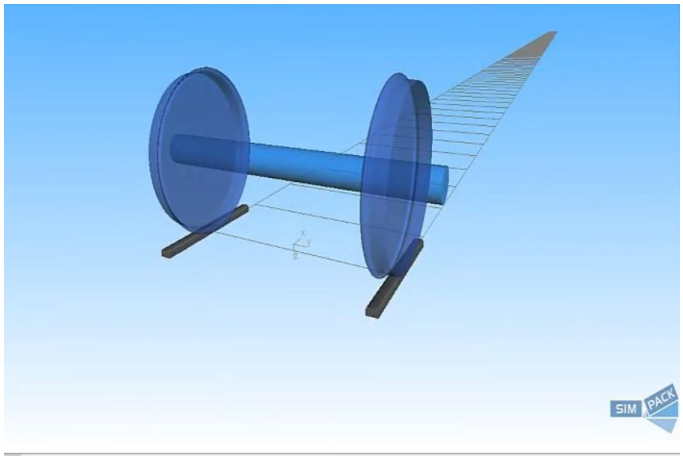

figure3. 2:The wheel and rail model

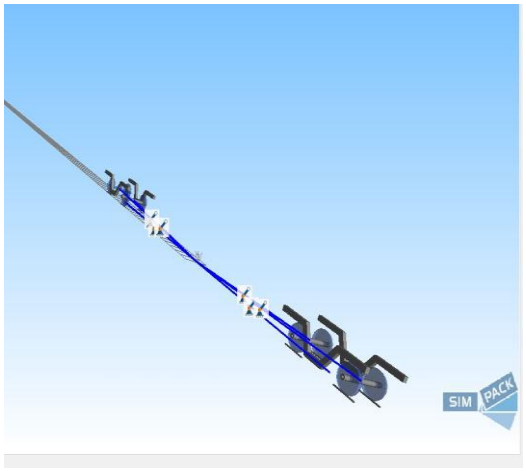

figure3. 3:The bogie frame assembly

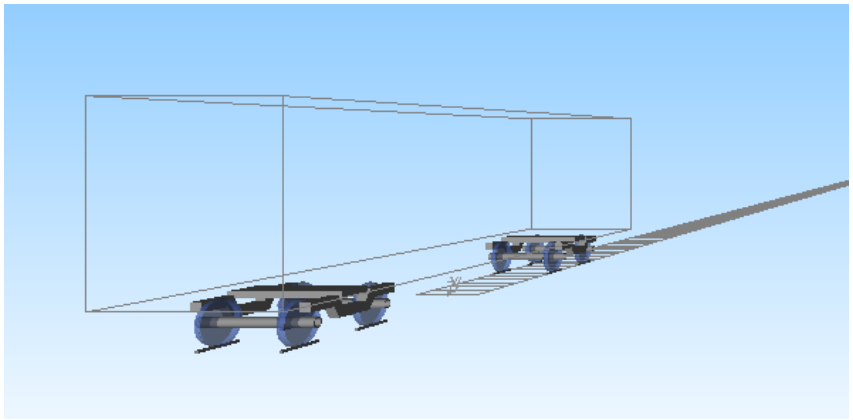

Figure3. 4:Final assembled Freight car body

Table 3. 1:Degree of freedom of each rigid body

Wagon Component	Horizontal	Lateral	Bounce	Yaw	Roll	Pitch
wagon frame	x_c	y_c	z_c	Ψ_c	θ_c	ϕ_c
Bolster 1	-	y_{bol1}	z_{bol1}	-	-	ϕ_{bol1}
Bolster2	-	y_{bol2}	z_{bol2}	-	-	$\phi_{bol\ 2}$
Wheelset 1	x_{w1}	y_{w1}	z_{w1}	ψ_{w1}	θ_{w1}	ϕ_{w1}
Wheelset 2	x_{w2}	y_{w2}	z_{w2}	Ψ_{w2}	θ_{w2}	ϕ_{w2}
Wheelset 3	x_{w3}	y_{w3}	z_{w3}	Ψ_{w3}	θ_{w3}	ϕ_{w3}
Wheelset 4	x_{w4}	y_{w4}	z_{w4}	Ψ_{w4}	Θ_{w4}	ϕ_{w4}
Bogie frame 1	x_{b1}	y_{b1}	z_{b1}	Ψ_{b1}	θ_{b1}	ϕ_{b1}
Bogie frame 2	x_{b2}	y_{b2}	z_{b2}	ψ_{b2}	Θ_{b2}	ϕ_{b2}

3.4: Analytical approach freight wagon multi-body dynamics

Analytical approach to dynamics includes: -

- Determination of creepage
- Determination of Creep force
- Determination of induced force and moment w/r contact
- Formulate an equation of motion

A. Determination of creepage

The relative motion between two bodies i and j that are in contact can be the result of rolling and sliding motion. In the general case of rolling and sliding, the two bodies have different velocities. The different angular velocities Ωi and Ω j or relative angular velocity along the normal to the surfaces at the contact point creates spin. On the other hand, velocities Vi and Vj at the contact point are not equal; the rolling motion is accompanied by a longitudinal and lateral slide

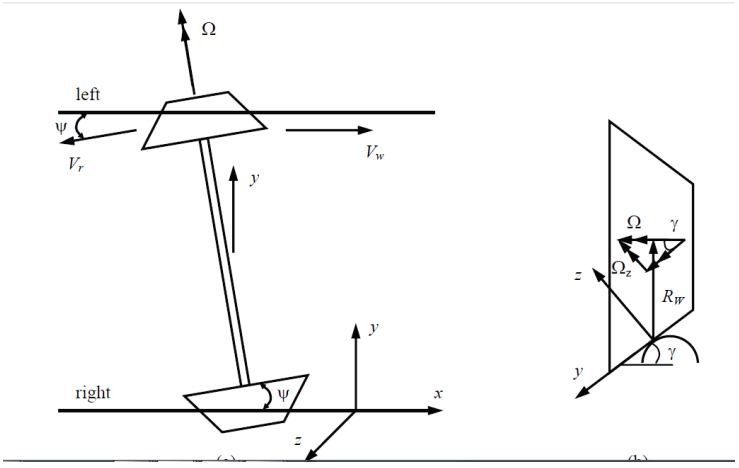

Figure3. 5: Wheelset Creepage[14]

Longitudinal creepage

$$s_{xi} = \frac{vx^{wi} - vx^{r}}{v} \qquad (3.1)$$

Where vx^{wi} and vx^{r} are longitudinal velocity for -wheelset and rail respectively,

V Designate mean velocity along the curve

I imply (1,2,3 and 4 Wheelset).

Equation (3.1)according to[47]

$$S_{XLi} = 1 - \left(\frac{r_L}{r_0}\right) + \frac{l_0 \cdot \dot{\Psi}_{wi}}{V} \qquad (3.2)$$

$$S_{XRi} = 1 - \left(\frac{r_r}{r_0}\right)_i - \frac{l_o \cdot \dot{\Psi}\ \dot{\Psi}_{wi}}{V} \qquad (3.3)$$

Lateral creepage

$$S_{Yi} = \frac{v_y^{wi} - v_y^r}{V} \tag{3.4}$$

According to[47] Equation lateral creepage can be expressed as

$$S_{YRi} = \left[\frac{\dot{Y}_{wi}}{V} - \Psi_{wi} \right] \left(\frac{r_r}{r_o} \right) + \frac{\dot{\theta}_{wi}}{V} \tag{3.5}$$

$$S_{YLi} = \left[\frac{\dot{y}_{wi}}{V} - \Psi_{wi} \right] \left(\frac{r_L}{r_o} \right)_i + \frac{\dot{\theta}_{wi}}{V} \tag{3.6}$$

Spin creepage

$$S_{ZLi} = \frac{\Omega_Z^{wi} - \Omega_Z^r}{V} \tag{3.7}$$

Where Ω_Z^{wi} and Ω_z^r designate spin creepage of the wheelset and rail along the z-axis respectively. According to Equation (3.7) Spin creepage for the left and right i wheelset derived to

$$S_{ZLi} = \frac{\dot{\Psi}_{wi}}{V} - \left(\frac{\gamma_L}{r_o} \right)_i \tag{3.8}$$

$$S_{Zr} = \frac{\Psi'_{wl}}{V} + \left(\frac{\gamma_r}{r_o} \right)_i \tag{3.9}$$

3.5: Archard's wear model in SIMPACK

The SIMPACK software offers the Archard wear model to calculate wear depth and wear distribution along wheel profiles. The Archard wear model is a function of the sliding distance, normal force, and hardness of the material. The wear volume of the material worn away is

proportional to the product of the sliding distance and the normal force and inversely proportional to the hardness of the worn material, as explained in Equation (2.10). The sliding distance and normal force, which are input to the Archard model to calculate wear depth, were obtained through vehicle modeling and dynamics calculations based on the FASTSIM algorithm.

To apply the wear model in SIMPACK, first define a result element of the Archard law for each wheel whose wear is to be determined, and the value of wear coefficients is filled based on the wear map described in chapter two figure (2.9), which is summarized in Table (3.2).

Wear coefficients are usually constant. However, there are three wear regimes: mild wear, severe wear, and seizure, each with its own set of wear coefficients. Mild wear is oxidative, resulting in the characteristic brown powder visible all along a train track. Small metal flakes peel away from the base material as a result of severe wear. Seizures destroy the material surface. When certain parameters change, such as when the relative velocity or pressure exceeds or falls below a given value, the transitions between wear regimes occur abruptly.

Table 3. 2:SIMPACK wear coefficients inputs[38]

(k2) mild 1	0.0005
(k4) mild 2	0.0005
(k3) severe	0.0035
(k1) seizure	0.035
The hardness of the material (N/m2)	3000000000
Relative velocity limit mild1-severe	0.2
Relative velocity limit severe-mild2	0.7
Relative hardness limit	0.8

3.6: Post-processing in MATLAB

The contact analysis in Simpack assumes a nonvarying rail profile in the contact area for Hertzian normal contact and steady-state tangential contact. All these assumptions are often applicable in simulations of dynamic vehicle–track interaction. However, during wear calculations, they may lead to a significant error. Therefore, to achieve an accurate calculation of the rail wear the contact is re-evaluated in a post-processing step using a MATLAB code. Given the wheel and rail contact geometries and the normal force and creepages from the Simpack simulation, the post-processing step in MATLAB provides a detailed wear removal estimation.

3.7: Profile updating

The updating method of the wheel profiles is a crucial point of the profile wear prediction model. Its objective is to determine the mileage after which wheel profiles should be updated and a new calculation of wheel/rail contact should be performed. According to comparisons of several approaches, the most effective wheel profile update strategy is based on the maximum wear depth, and the profile is updated when a given threshold of the maximum value of cumulative wear depth is reached.

3.8: Post Processing

The SIMPACK post-process program generates detailed results for each body forming the multi-body model in the railway vehicle. Based on this procedure wear depth results from wear calculation are plotted for each scenario. Finally based on the extracted data, evaluation and discussion of the specific objective function of the study will be performed.

Chapter4: RESULT AND DISCUSSION

4.1: Introduction

In this chapter, the simulated wheel wear result will be visualized by evaluating the wear depth influence of different parameters like curve radius, curving speed, superelevation, and on wear along different curves will be addressed. The results of the first wheelset that is to say the right and left wheels will be analysed and the third wheelset will be analysed for some scenarios

4.2: Effect of curve Radius

The curve radius in the simulations varied from 800 to 1200 m and the super-elevation values ranged from 0.06 to 0.03m, which represent the narrowest and the largest curve, respectively. The speed of the train was fixed at 60 km/h for all the curves considered. The track has got curves of up to 500m but for a better analysis, narrow curves were considered because they bring out the maximum impact of the cases considered.

The vehicle is assumed to run on a straight track first, then on a bloss transition curve before entering a circular curve, and then on a bloss transition curve and straight line in the final stage, with the total distance corresponding to the radius shown in Table 4.2

Table 4. 1:Sebeta to Meiso phase 1 project curve length technical parameters.

Curve Radius(m)	Length(m)
600	190
800	180
1000	140
1200	120

At the same safe curving speed v = 60 km/h, with a balanced gradient of 1/40 track curves of 600m,800m,100m, and 1200m were analysed and their corresponding superelevation was calculated according to the equation below.

$$superelevation = \frac{GV^2}{127R} \quad (4.1)$$

Where,

G=track gauge length (mm)

v=velocity (km/hr.)

R=Radius of curvature (m)

The simulation analysis conducted under the corresponding characteristic curves is shown in Table.

Table 4. 2:Curve parameters with calculated superelevation

Curve Radius Variation	Calculated superelevation(m)
600m	0.06
800m	0.05
1000m	0.04
1200m	0.03

Using the above parameters four simulations were carried out and the corresponding longitudinal creep forces and derailment coefficient were recorded. In the notations, WS1R and WS1L indicate the right and left wheels of the first wheelset of the front bogie frame respectively

Table 4. 3:Simulated results at 600,800,1000 and 1200m curve Radius

V=40km/hr., cant (α_t) =1/40	Wheelset	R=600m	R=800m	R=1000m	R=1200m
Longitudinal creep force (kN)	W1SR	13.4	13.2	12.8	12.4
	W1SL	18.2	17.2	16.4	15.6
Lateral force (kN)	W1SR	6.4	4.9	4	3.5
	W1SL	13.9	12.7	11.1	9
Derailment coefficient	W1SR	0.1	0.08	0.07	0.07
	W1SL	0.28	0.25	0.2	0.1
Wear volume(m)	W1SR	0.0063	0.0055	0.0045	0.0032
	W1SL	0.0068	0.006	0.0049	0.0036

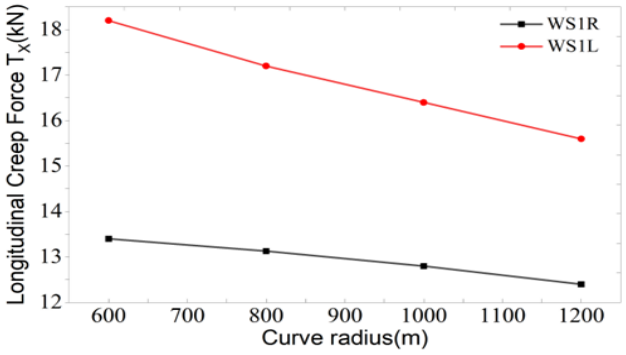

(a)

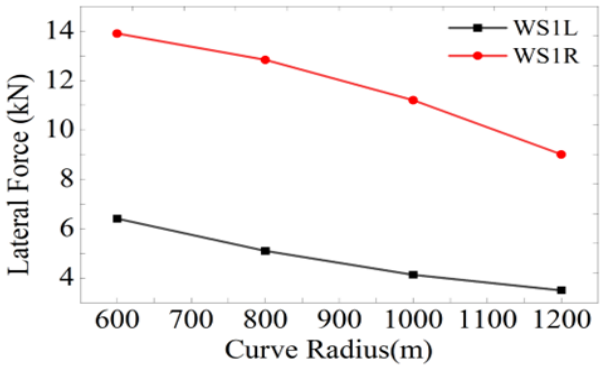

(b)

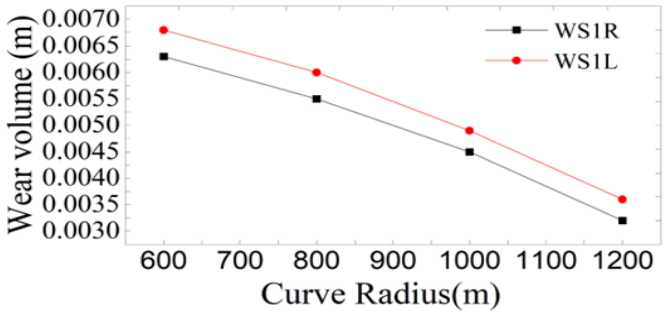

(c)

Figure 4. 1 Effect of curve radius on wear.

The lateral forces and longitudinal creep forces are very high on the left wheel of the leading wheelset when the curve radius is small which indicates there are high stresses on small curves which also leads to high wear volumes removal of 6.8mm. However, as the curve radius increases from 600m to 1200m the wheel-rail lateral force, longitudinal creep forces, and wear volume reduce accordingly as seen in Figures 4.1a and 4.1b.

Figure 4.1c above observed that the creep forces of the left wheel are higher (18.5kN) compared to that of the right wheel(13.5kN) this is because as a train enters the curve, wheel–rail interaction is intensified by 'irregularity' (railway alignment design), and the wear increases. As the train pulls out of the curve, the influence of 'irregularity' on the wheel rail interaction decreases and the wear is alleviated. According to YanjieWu found that when the curve radius is less than 800 m, the curve radius has a significant influence on rail wear. Additionally, the length of the transition curve also has an impact on rail wear.

4.3: Effect of curving speed

Using a curving peed of 40,60,80 and 100 km/respectively when the vehicle passes the center of the curved track some of the variations of the parameters, concerning the behavior of the wheelset and track, are listed in Table.

Table 4. 4: Simulated results of the influence of speed on curved track

R=1000m, (α_t) =1/40	Wheelset	40km/hr.	60km/hr.	80km/h	100km/hr.
Lateral creep force (kN)	WSIR	-8.7	-5.9	-3.4	-1.5
	WS1L	-7.3	-5.5	-4	-2.7
	WS2R	6.2	7.9	9.6	11.2
	WS2L	10.2	11.5	10.1	14.1
Normal Load (kN)	WS1R	64.5	58.4	53.3	49.3
	WS1L	67.7	72.4	66.8	80.5
	WS2R	66.2	68.5	71.3	74.6
	WS2L	68.4	62.7	57.1	74.6
Derailment coefficient	WS1R	0.12	0.13	0.14	0.16
	WS1L	0.18	0.2	0.23	0.25
	WS1R	0.0036	0.003	0.006	0..68

Wear Volume(m)	WS1L	0.0065	0.006	0.007	0.0078
	WS2R	0.0026	0.0024	0.0032	0.004
	WS2L	0.0052	0.005	0.006	0.0068

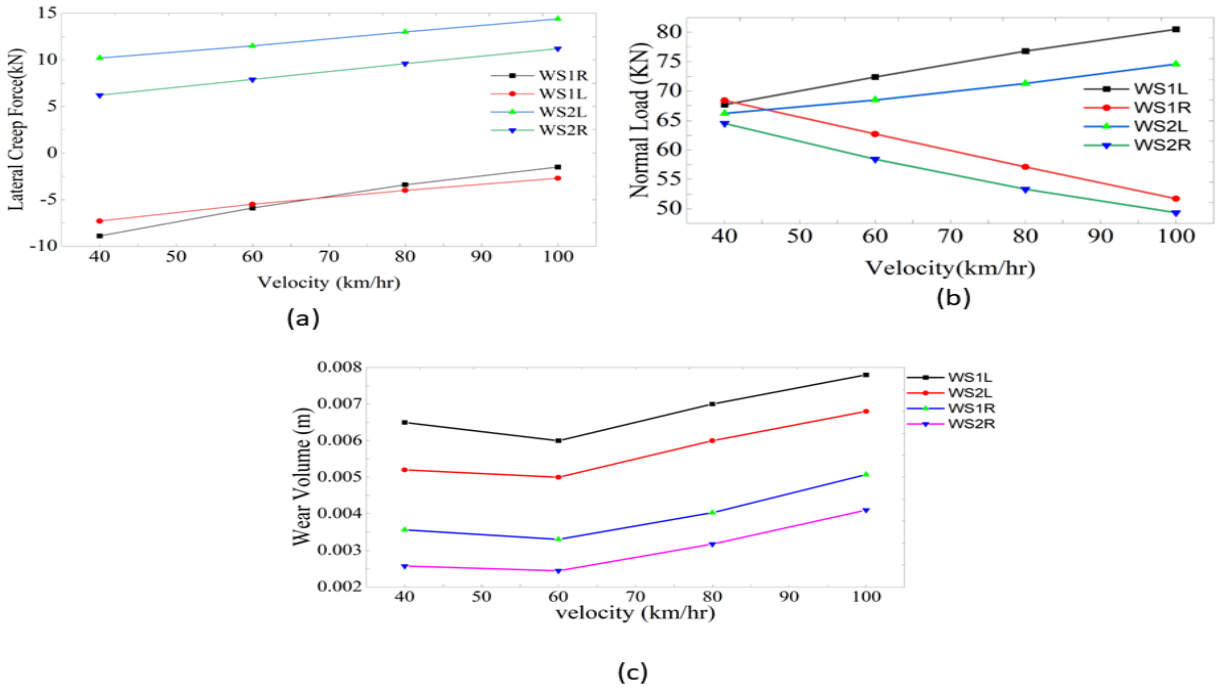

Figure 4. 2: Effects of speed on wear on curved track

From Figure 4.4, the difference between the normal loads of the left and right wheels increases with increasing curving speed. This is mainly caused by the increasing of the centrifugal force of the vehicle due to the increased curving speed. When the speed increases from 40 to 100 km/h, the total lateral creep force of the leading wheelset (WS1L) increases hence leading to an increase in wear volume of 7.8mm. The lateral force is caused by the curved track, and in the opposite direction of the Y-axis. A common trend can be found where the wear first increases and then decreases. This tendency is the result of the fluctuation of wheel–rail forces throughout the curve.

The rail wear caused by the outside wheels (WS1L and WS2L) decreases with the speed increasing from 40 to 60 km/hr. and increases from 60 to 100 km/h. The wear caused by wheels (WS1R and WS2R) grows with increasing speed. For the cases of the different speeds varied, the rail wear volume caused by WS1L is the largest and continues to increase with further increasing the speed. But, the increase of the curving speed is limited by the super-elevation of the curve track. Otherwise, the difference between the normal loads on the left and right wheels of the same wheelset further increases.

4.4: Effect of superelevation of wear.

In the efforts of improving wear along the curve, optimizing the sizes of the track is a good measure. Analysis was carried out when the curving speed is v=60 km/h. The super-elevation h_t is selected as 80, 100, and 120mm, respectively.

Table 4. 5: simulated results under selected super elevations

V=60km/h, α_t=1/40	Wheelset	ht=80mm	ht=100mm	ht=120mm	ht=140mm
Normal load (kN)	WS1L	60.5	59.2	58.5	55.6
	WS3L	57.3	56.5	54.7	52.7
	WS1R	36.2	37.8	38.3	36.0
	WS3R	32.5	33.6	34.8	38.9
Wear volume(m)	WS1R	0.003	0.0026	0.0022	0.0017
	WS1L	0.007	0.0068	0.0065	0.006
	WS3R	0.0026	0.0022	0.0018	0.0014
	WS3L	0.0068	0.0064	0.0059	0.0054

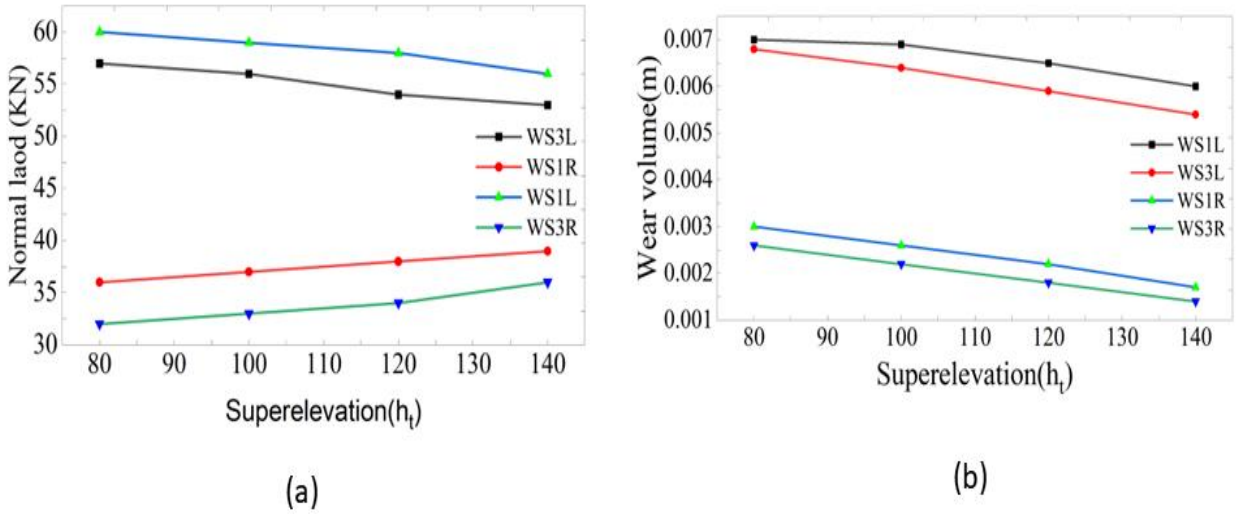

Figure 4. 3:Effect of super elevation on wear

From Figure 4.3b on reducing ht the WS1L and WS3L or the outside wheels of the leading wheelset dominate the wear as seen from the high loads experienced that lead to a high wear volume of 7.1mm and 6.7mm respectively. This is because of the centrifugal force that pushes the wheelset outward hence increasing the creep forces and wear. However, the normal loads of the left wheels (WS1L and WS3L) decrease linearly with increasing ht hence reducing the wear depth to around 7.1mm and 6.7mm respectively. According to Minhao Zhu found that increasing the track super-elevation efficiently lowers the normal load difference between the left and right wheels of the front wheelset, as well as the contact stresses and wear.

4.5: Validation

The work carried out by Li et al. [42]was used to validate the result. The wear depth in the contact patch was based on Archard's model and extensive field measurements of the wheel/rail profile were carried out on the curves of the on different curves but the main analysis was carried out on the 500m curve radius because its wear is more serious than the rest. The field results indicated that a max wear depth of 9mm was realized after a distance of 200,000km which is close to the results of 6.8mm obtained when the curve radius used was 600m and a running

distance of 20,000km These differences are mainly induced by many factors such as track irregularities, friction coefficient, longitudinal slop, traction, braking, etc.

Chapter5: CONCLUSION, RECOMMENDATION, AND FUTURE WORK

5.1: Recommendation

To minimize wear, railways should implement curve-specific speed restrictions for freight trains based on radius, cant deficiency. Finally, equilibrium cant should be maintained through regular profiling and alignment to reduce flange impacts. Implementing these recommendations will enhance wheel life, reduce maintenance costs, and improve safety.

5.2: Future work

To extend this research, future work could incorporate more diverse train types and a broader range of curving conditions into the models. More complex simulation of stresses and fatigue using finite element methods would also enhance understanding of wear mechanisms. Validation through physical testing and cost-benefit analyses of infrastructure upgrades should be pursued. Effects of additional factors like traction forces, lubrication, track stiffness, and defects represent important areas for further study. Overall, the thesis will provide a solid framework, but there is significant scope for advancing the models, insights, and practical guidance by expanding the parameters and detail of analysis in future work

5.3: Conclusion

Under this research, a model was developed to predict the wear of Ethio-Djibouti freight car wheels under different curve parameters and the model was based on vehicle multibody dynamic analysis in which all the bodies were considered rigid. The following was found out after analysis.

The research conclusively demonstrates that tighter curve radii, insufficient cant, and higher curving speeds result in exponentially higher wheel wear rates for freight trains. There are diminishing returns when increasing cant beyond equilibrium. Optimized speed restriction and ideal cant deficiency based on radius and traction can reduce wear. The validated wear prediction model provides an important tool for railway maintenance planning and traffic management to minimize wheel-rail wear in curves.

Chapter6: References

[1] R. Pankhurst, “The Franco-Ethiopian railway and its history,” *Ethiop. Obs.*, vol. 6, no. 4, pp. 342–379, 1963.

[2] L. Wang, “Microstructure and Residual Stress State in the Contact Zone of Rails and Wheels,” no. September, 2002.

[3] Global Infrastructure Hub, “Addis Ababa – Djibouti Railway,” *Glob. Infrastruct. Hub*, no. January 2018, pp. 72–77, 2020, [Online]. Available: https://www.gihub.org/resources/showcase-projects/addis-ababa-djibouti-railway/

[4] M. Kozicki, “The history of railway in Ethiopia and its role in the economic and social development of this country,” *Stud. Dep. African Lang. Cult.*, no. 49, 2015.

[5] T. Jendel and M. Berg, “Prediction of Wheel Profile Wear,” vol. 3114, no. March, 2016, doi: 10.1080/00423114.2002.11666258.

[6] A. Zmitrowicz, “WEAR PATTERNS AND LAWS OF WEAR – A REVIEW Alfred Zmitrowicz,” no. 1803, pp. 219–253, 2006.

[7] J. Tunna, J. Sinclair, and J. Perez, “Proceedings of the Institution of Mechanical Engineers , Part F : Journal of Rail and Rapid Transit,” 2007, doi: 10.1243/0954409JRRT72.

[8] X. Jin, “Research Progress of High-Speed Wheel – Rail Relationship,” 2022.

[9] Y. Ye, Y. Sun, S. Dongfang, D. Shi, and M. Hecht, *Optimizing wheel profiles and suspensions for railway vehicles operating on specific lines to reduce wheel wear : a case study*. The Author(s), 2021. doi: 10.1007/s11044-020-09722-4.

[10] S. Jung-won, K. Seok-jin, J. Hyun-kyu, and L. Chan-woo, “ce pt us,” *Tribol. Trans.*, 2019, doi: 10.1080/10402004.2019.1588446.

[11] Y. Lu, Y. Yang, J. Wang, and B. Zhu, “Optimization and Design of a Railway Wheel Profile Based on Interval Uncertainty to Reduce Circular Wear,” vol. 2020, 2020.

[12] H. Tobias, P. Stief, J. Dantan, A. Etienne, and A. Siadat, “curve based online assessment for Wear based online assessment.,” *Procedia CIRP*, vol. 88, pp. 312–317, 2019, doi: 10.1016/j.procir.2020.05.054.

[13] S. Yaseen and T. Wani, “Design and Analysis of a Railway Bogie Truck,” *Int. J. Ignited Minds*, vol. 01, no. 06, pp. 13–19, 2014.

[14] W. Rail and I. Optimisation, *Wheel/Rail Interface Optimisation*.

[15] S. Iwnicki, *Handbook of Railway Vehicle Dynamics*.

[16] W. Zhai, J. Gao, P. Liu, and K. Wang, “Reducing rail side wear on heavy-haul railway curves based on wheel-rail dynamic interaction,” *Veh. Syst. Dyn.*, vol. 52, no. SUPPL. 1, pp. 440–454, 2014, doi: 10.1080/00423114.2014.906633.

[17] K. Wang, C. Huang, W. Zhai, P. Liu, and S. Wang, “Progress on wheel-rail dynamic performance of railway curve negotiation,” *J. Traffic Transp. Eng.*, vol. 1, no. 3, pp. 209–220, 2014, doi: 10.1016/S2095-7564(15)30104-5.

[18] F. Of and R. Vehicle, *No Title*.

[19] P. D. Hargreaves, “Queensland University of Technology School of Engineering Systems DEVELOPMENT OF AN INTEGRATED MODEL FOR ASSESSMENT OF OPERATIONAL RISKS IN Associate Supervisor :,” 2007.

[20] J. Wang, X. Chen, X. Li, and Y. Wu, “In fl uence of heavy haul railway curve parameters on rail wear,” *EFA*, vol. 57, pp. 511–520, 2015, doi: 10.1016/j.engfailanal.2015.08.021.

[21] M. S. Sichani, *On Efficient Modelling of Wheel-Rail Contact in Vehicle Dynamics Simulation*. 2016.

[22] B. Dirks, *Simulation and measurement of wheel on rail fatigue and wear*. 2015.

[23] A.Ekberg, “Rolling contact Fatigue of Railway wheels.pdf.” 2016.

[24] K. Tatsumi, T. Mineyasu, and H. Minoru, “Development of SP3 Rail with High Wear Resistance and Rolling Contact Fatigue Resistance for Heavy Haul Railways †,” vol. 16, no. 16, pp. 32–37, 2011.

[25] Intergovernmental Organisation for International Carriage by Rail, “Status : IN FORCE APTU Uniform Rules (Appendix F to COTIF 1999) Uniform Technical Prescriptions (UTP) relating to the Subsystem Rolling Stock FREIGHT WAGONS,” vol. 06, no. December 2010, pp. 2011–2013, 2012.

[26] A. Sladkowski and M. Sitarz, “Analysis of wheel – rail interaction using FE software,” vol. 258, no. December 2003, pp. 1217–1223, 2005, doi: 10.1016/j.wear.2004.03.032.

[27] P. Taylor and H. Wu, “Vehicle System Dynamics : International Journal of Vehicle Mechanics and Effects of wheel and rail profiles on vehicle performance,” no. February 2014, pp. 37–41, 2007, doi: 10.1080/00423110600875393.

[28] T. Tomioka, T. Takigami, and Y. Suzuki, “Numerical analysis of three-dimensional flexural vibration of railway vehicle car body,” *Veh. Syst. Dyn.*, vol. 44, no. SUPPL. 1, pp. 272–285, 2006, doi: 10.1080/00423110600871301.

[29] W. ZHONG, W. J. Wang, and Q. Y. Liu, “Effect of curve radius on rolling contact fatigue properties of rails,” *J. Southwest Jiaotong Univ.*, vol. 44, no. 2, pp. 254–257, 2009.

[30] P. Turabimana and C. Nkundineza, “Development of an On-Board Measurement System for Railway Vehicle Wheel Flange Wear,” 2020.

[31] J. F. Archard and P. R. S. L. A, “Elastic deformation and the laws of friction,” *Proc. R. Soc. London. Ser. A. Math. Phys. Sci.*, vol. 243, no. 1233, pp. 190–205, 1957, doi: 10.1098/rspa.1957.0214.

[32] I. A. Soldatenkov, “Evolution of contact pressure during wear of the coating in a thrust sliding bearing,” *J. Frict. Wear*, vol. 31, no. 2, pp. 102–106, 2010, doi: 10.3103/S1068366610020029.

[33] F. Informa *et al.*, “Vehicle System Dynamics : International Journal of Vehicle Mechanics and Mobility A Lateral Semi-Active Damping System For Trains,” no. April 2013, pp. 37–41, 2007.

[34] S. Fundamentals, *Encyclopedia of Tribology*. 2013. doi: 10.1007/978-0-387-92897-5.

[35] Y. Muhamedsalih, J. Stow, and A. Bevan, “Use of railway wheel wear and damage prediction tools to improve maintenance efficiency through the use of economic tyre turning,” *Proc. Inst. Mech. Eng. Part F J. Rail Rapid Transit*, vol. 233, no. 1, pp. 103–117, 2019, doi: 10.1177/0954409718781127.

[36] J. Santamaria, E. G. Vadillo, and O. Oyarzabal, “Wheel-rail wear index prediction considering multiple contact patches Wheel-rail wear index prediction considering multiple contact patches,” vol. 267, pp. 1100–1104, 2009, doi: 10.1016/j.wear.2008.12.040.

[37] J. Lundmark, “Rail Grinding and its impact on the wear of Wheels and Rails,” 2007.

[38] R. Lundén and B. Paulsson, *Introduction to wheel-rail interface research*. Woodhead Publishing Limited, 2009. doi: 10.1533/9781845696788.1.3.

[39] Y. Ye and Y. Sun, “Reducing wheel wear from the perspective of rail track layout optimization,” *Proc. Inst. Mech. Eng. Part K J. Multi-body Dyn.*, vol. 235, no. 2, pp. 217–234, 2021, doi: 10.1177/1464419320956831.

[40] O. Arias-Cuevas, Z. Li, R. I. Popovici, and D. J. Schipper, “Simulation of curving behaviour under high traction in lubricated wheel-rail contacts,” *Veh. Syst. Dyn.*, vol. 48, no. SUPPL. 1, pp. 299–316, 2010, doi: 10.1080/00423111003746132.

[41] D. V. Gutsulyak, L. J. E. Stanlake, and H. Qi, “Twin disc evaluation of third body materials in the wheel/rail interface,” *Tribol. - Mater. Surfaces Interfaces*, vol. 15, no. 2, pp. 115–126, 2021, doi: 10.1080/17515831.2020.1829878.

[42] X. Li, T. Yang, J. Zhang, Y. Cao, Z. Wen, and X. Jin, “Rail wear on the curve of a heavy haul line—Numerical simulations and comparison with field measurements,” *Wear*, vol. 366–367, pp. 131–138, 2016, doi: 10.1016/j.wear.2016.06.024.

[43] J. Yang, H. Song, L. Fu, M. Wang, and W. Li, “A new solution method for wheel / rail rolling contact,” *Springerplus*, 2016, doi: 10.1186/s40064-016-2128-2.

[44] T. Telliskivi and U. Olofsson, “Contact mechanics analysis of measured wheel – rail,” vol. 215, pp. 65–72, 2015.

[45] U. Olofsson and S. Bjorklund, “Simulation of mild wear in boundary lubricated spherical roller thrust bearings,” pp. 180–185, 2000.

[46] Z. Guotang and Z. Shugu, “Effect of curve radius and off-balance superelevation on side wear of high rail on curved track [J],” *China Railw. Sci.*, vol. 16, no. 3, pp. 90–95, 1995.

[47] J. Pombo, “Application of a Computational Tool to Study the Influence of Worn Wheels on Railway Vehicle Dynamics,” *J. Softw. Eng. Appl.*, vol. 05, no. 02, pp. 51–61, 2012, doi: 10.4236/jsea.2012.52009.

Chapter7: Appendix

Appendix A: Bogie side frame dimensions

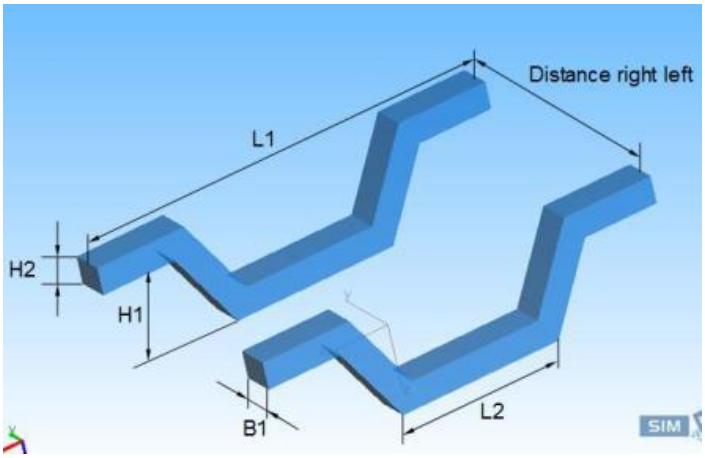

Length L1	Length L2	Height H1	Height H2	Width B1 Distance right left
2.2m	0.8m	0.23m	0.19m	0.2m

Appendix B: Dummy dimensions

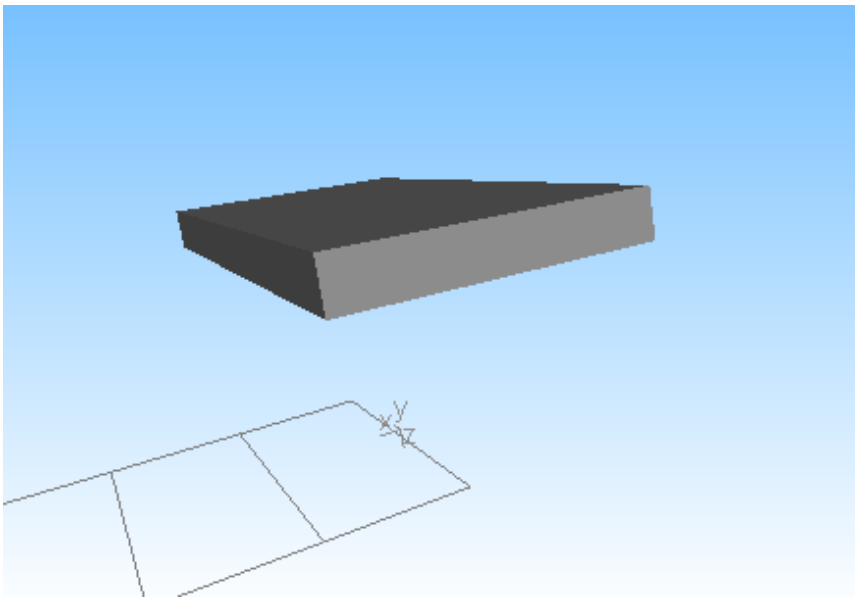

Type	Length x	Length y	Length z
Cuboid	0.65m	2.2m	0.14m

Appendix C: Design Parameter Specifications of the Ethio Djibouti Freight Train.

Parameter	symbol	**Value**
suspension		
longitudinal stiffness Ps	$k_{X,}$	5450000
Lateral stiffness Ps	$k_{Y,}$	5450000
Vertical stiffness Ps	k_z	9000000
longitudinal damping Ps	c_x	5000 N/m
lateral damping Ps	c_y	5000 N/m

vertical damping Ps	c_z	10500 N/m
longitudinal stiffness SS	$k_{X,}$	130000 N/m
Lateral stiffness SS	$k_{Y,}$	130000 N/m
Vertical stiffness SS	k_z	240000 N/m
longitudinal damping SS	c_x	15000 N/m
lateral damping SS	c_y	15000 N/m
vertical damping SS	c_z	25000 N/m
Parameter	symbol	**Value**
Carbody		
Carbody mass	mc	24800
Roll moment of inertial	I_{XX}	96000 kgm^2
Pitch moment of inertial	I_{YY}	1700000
yaw moment of inertial	I_{ZZ}	1650000
Bogie Frame		
Bogie frame Mass	Mb	47000 kgm^2
Roll moment of inertial	I_{XX}	2100 kgm^2
Pitch moment of inertial	I_{YY}	2600 kgm^2
yaw moment of inertial	I_{ZZ}	4000 kgm^2
Wheelset		
Wheelset Mass	Mw	1800 kgm^2
Roll moment of inertial	I_{XX}	800 kgm^2
Pitch moment of inertial	I_{YY}	140 kgm^2
yaw moment of inertial	I_{ZZ}	800 kgm^2

Appendix D: Technical Parameters of the Ethio Djibouti Freight Train

Technical parameter	Description
model	Cw4 open-top wagon
Bogie configuration	Bo-Bo
Length of a single wagon	13976 mm
Length between Bogie centers	9210 mm
Minimum negotiable Radius	100mm
Length inside the car body	13000 mm
Width inside the car body	2890 mm
Height inside the car body	2075 mm

Appendix E: Worn Right wheel

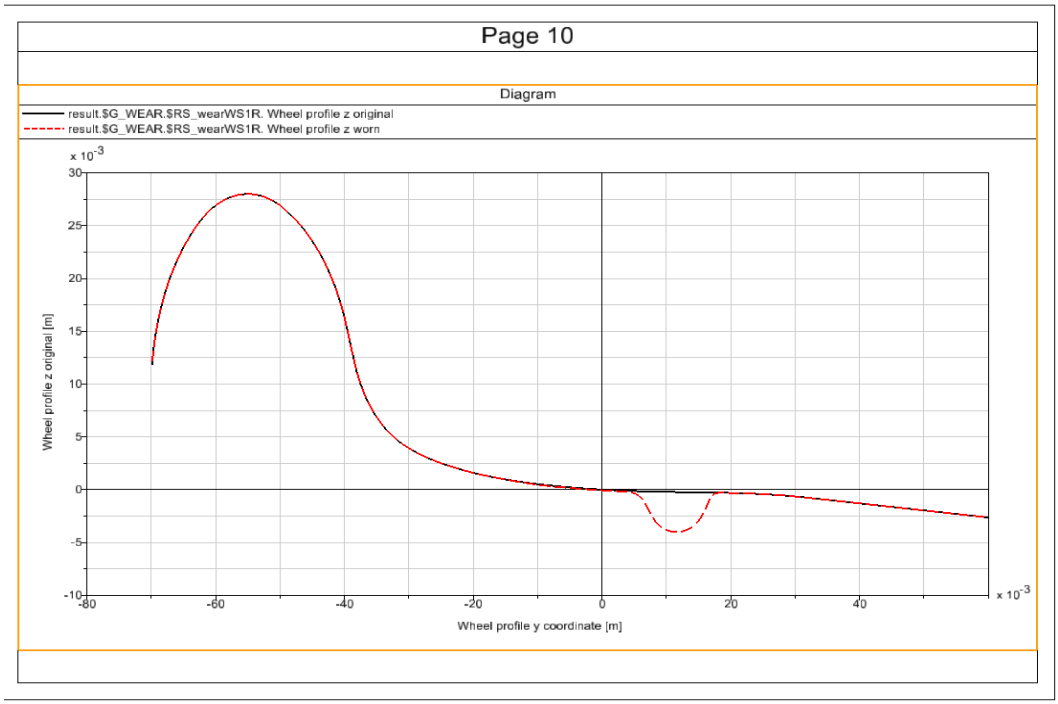

Appendix F: Worn Left wheel

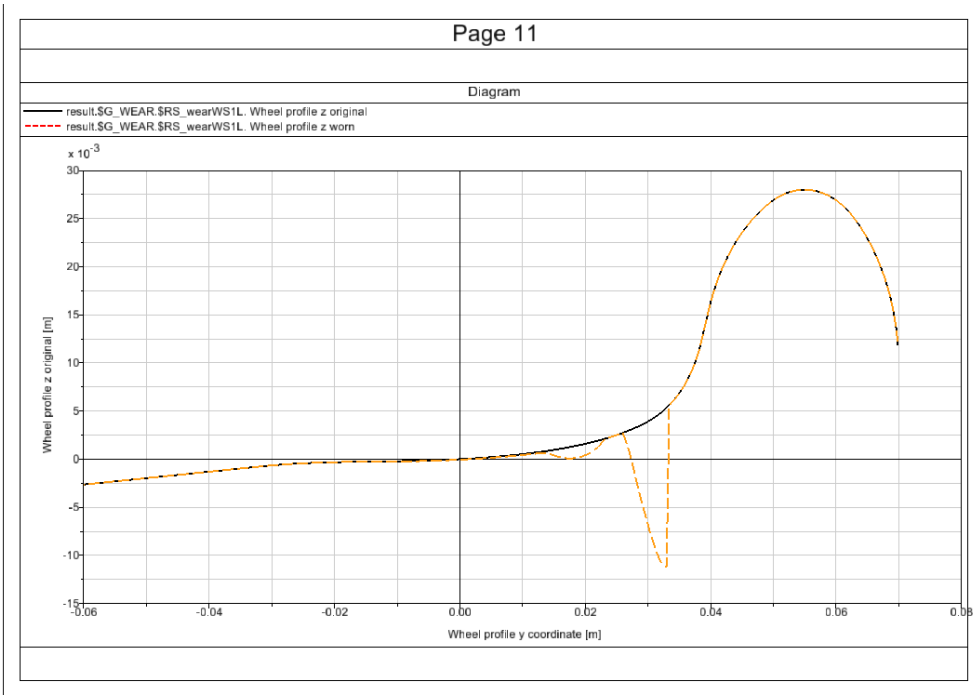

Appendix G: Technical parameters of Sebeta-Adama project

III Technical Parameters

Main technical parameters for the Project are determined as follows through negotiation with Ethiopian Railways Corporation:

Scope	SEBETA – ADAMA (including)	ADAMA (excluding) – MIESO (including)
Gauge	1435mm	1435mm
Number of main line	Double tracks	Single track
Speed target value	120km/h	120 km/h
Min. radius of curve	800m	800m
Maximum gradient	Ruling grade: 9‰, pusher grade: 18.5‰	Ruling grade: 9‰, pusher grade: 18.5‰
Type of traction	Electric power	Electric power
Type of locomotive	Passenger train, freight train HXD3B	Passenger train, freight train HXD3B
Traction mass	3500T	3500T
Length of receiving-departure track	850m (880m for dual-locomotive)	850m (880m for dual-locomotive)
Distance between centers of tracks	4.0m	/
Block system	Automatic inter-station block	Automatic inter-station block

IV Engineering Measures and Equipment Arrangement

EPC quotation for the Project aims at construction of a standard-gauge railway applicable to current national conditions of Ethiopia based on the concept of localization of civil engineering measures and applicability of equipment arrangement.

(I) Division of sections and units

1 Double-track section

SEBETA-ADAMA (including), AK0+000-AK116+650; divided into two units:

Unit 1: SEBETA-LABU, AK0+000-AK14+800

Unit 2: LABU-ADAMA, AK14+800-AK116+650

2 Single-track section

ADAMA (excluding) – MIESO, AK116+650-CK342+900; divided into one unit:

Unit 3: ADAMA-MIESO, AK116+650-CK342+900

2

Appendix H: Technical parameters of Sebeta-Adama project showing various Curves

(III) **Line**

1 Line scheme

See 1:50,000 plan of the line scheme.

2 Plane and profile design of the line

(1)Plane design

1) Min. radius of curve: generally 800m, 600m in case of difficulties.

2) Length of transition curve

Length of transition curve

Radius of curve (m)	Common length (m)
5000	40
4500	40
4000	50
3500	50
3000	50
2800	60
2500	60
2000	70
1800	80
1600	90
1400	100
1200	120
1000	140
800	180
600	190

3) Intermediate straight line and circular curve

Minimum length is 80m.

4) Distance between centers of tracks

The distance between centers of tracks of the main line in the double-track section shall be 4.0m, the curve section shall be based on the left line, and the right line shall be designed as a circle concentric with the left line; the distance between centers of tracks in the curve section shall be widened.

(2)Profile design

1) Gradient: ruling grade: 9‰, pusher grade: 18.5‰

6

Appendix I: technical parameters showing various speeds

EDR Speed Limit Order			
S.No	Comm NO	Speed Limit Kilo - Meter	Speed limit
1	7#	INDODE - BISHOFTU k52+744--52+844	25
2	526#	INDODE - LABU K16+441--K18+041	25
3	526#	MIESSO - DIREDAWA k379+000--k379+600	25
4	526#	MIESSO - DIREDAWA k380+247--k381+847	25
5	216#	ARAWA-ADIGALA K510+300--K530+300	40
6	216#	ARAWA-ADIGALA K530+300--K531+000	35
7	216#	ADIGALA -AYSHA K531+000--K610+400	40
8	5#	BIKE-DIREDAWA K414+782--K415+000	25
9	623	DIREDAWA-ARAWA K470+000--K475+000	35
10	623	INDODE-BISHOFTU K34+000--62+000	45
11	623	INDODE-BISHOFTU K62+000--112+830	50
12	25#	ADIGALA- DAWALE k550+000--k646+500	客车限60
13	25#	DIREDAWA- ARAWA K487+000--K537+200	客车限60
14	25#	ARAWA- ADIGALA k544+000---550+000	客车限60
15	25#	ARAWA- ADIGALA k537+200--544+000	客车限60
16	25#	DIREDAWA- ARAWA K462+235--487+000	55
17	25#	DAWALE -NAGAD K646+500--K656+700	50
18	25#	MIESSO - DIREDAWA k365+300--k367+300	45
19	25#	DAWALE -NAGADK656+700--K743+870	60
20	24#	METEHARA - SIRBAKUNKA k272+000--k277+000	40
21	24#	DIREDAWA- ARAWAK462+000--K464+000	40
22	24#	INDODE - BISHOFTU K42+000--46+000	40
23	24#	INDODE - LABUK17+000--K21+000	40
24	24#	BIKE- DIREDAWAK430+000--444+000	40
25	24#	ADIGALA - DAWALE K510+300--605+400	45
26	24#	INDODE - BISHOFTU k35+600--53+500	40
27	623	ADAMA - DIREDAWA K112+830--K462+235	50
28	623	METEHARA - SIRBAKUNKAk245+200--k247+500	35
29	208	INDODE - BISHOFTU K41+800--42+400	25
30	214	INDODE - BISHOFTU K58+00--K59+00	35
31	215	DIREDAWA- ARAWA K479+800--K480+800	